

RSC Advances



This is an *Accepted Manuscript*, which has been through the Royal Society of Chemistry peer review process and has been accepted for publication.

Accepted Manuscripts are published online shortly after acceptance, before technical editing, formatting and proof reading. Using this free service, authors can make their results available to the community, in citable form, before we publish the edited article. This *Accepted Manuscript* will be replaced by the edited, formatted and paginated article as soon as this is available.

You can find more information about *Accepted Manuscripts* in the [Information for Authors](#).

Please note that technical editing may introduce minor changes to the text and/or graphics, which may alter content. The journal's standard [Terms & Conditions](#) and the [Ethical guidelines](#) still apply. In no event shall the Royal Society of Chemistry be held responsible for any errors or omissions in this *Accepted Manuscript* or any consequences arising from the use of any information it contains.

Cite this: DOI: 10.1039/c0xx00000x

www.rsc.org/xxxxxx

PAPER

Highly Sulfonated Graphene and Graphene Oxide Nanosheets as Heterogeneous Nanocatalysts in Green Synthesis of Bisphenolic Antioxidants under Solvent Free Conditions

Hossein Naeimi*, Mohsen Golestanzadeh

Department of Organic Chemistry, Faculty of Chemistry, University of Kashan, Kashan, 87317-51167, Islamic Republic of Iran
 Email: *naeimi@kashanu.ac.ir*; Tel: +983155912388; Fax: +983155912397

Received (in XXX, XXX) Xth XXXXXXXXXX 20XX, Accepted Xth XXXXXXXXXX 20XX
 DOI: 10.1039/b000000x

Sulfonated functionalized graphene and graphene oxide nanosheets were prepared via chemical approaches and their catalytic activities were investigated in the green synthesis of 6,6'-(arylmethylene)bis(2,4-dialkylphenol) antioxidants. In this research, three types of the catalysts including sulfonated reduced graphene oxide nanosheets (catalyst **1a**), sulfonated graphene oxide nanosheets (catalyst **1b**), and sulfonated propylsilane graphene oxide nanosheets (catalyst **1c**) were synthesized and used in the synthesis of target molecules. The catalysts were characterized by field emission scanning electron microscopy (FE-SEM), transmission electron microscopy (TEM), atomic force microscopy (AFM), Fourier transform infrared spectroscopy (FT-IR), Raman spectroscopy, X-ray diffraction spectroscopy (XRD), and back acid-base titration. The catalyst **1a** showed excellent catalytic activity in the green synthesis of 6,6'-(arylmethylene)bis(2,4-dialkylphenol) antioxidants under solvent free conditions and reused several times without any appreciable loss of its catalytic activity even after eight consecutive cycles. In addition, high yield of the products, non-toxicity of the catalysts are other worthwhile advantages of the present methods.

Introduction

Phytochemicals are bioactive non-nutrient compounds found in plants. The most important class of phytochemicals in plant food sources is the group of phenolic compounds. Phenols especially polyphenols are very important materials in food and organic chemistry. These materials have been used as dyes,^{1,2} protecting groups for nucleosides,³ carbohydrates,⁴ anticancer drugs,⁵ epoxy resins,⁶ and antioxidants.⁷⁻¹² Phenolic antioxidants act as efficient free radicals scavengers by donating their alcoholic hydrogen or one of their delocalized electrons. In addition, the polyphenols have many industrial applications, for example they may be used as natural colorant, food preservatives, and paints, paper, and cosmetic production.¹³ Bisphenolic antioxidants are an important class of polyphenolic antioxidants. These antioxidants are usually manufactured by an acid catalyzed condensation reaction of

carbonyl and aromatic compounds. The chemical structures of some phenolic antioxidants are shown in Figure 1.

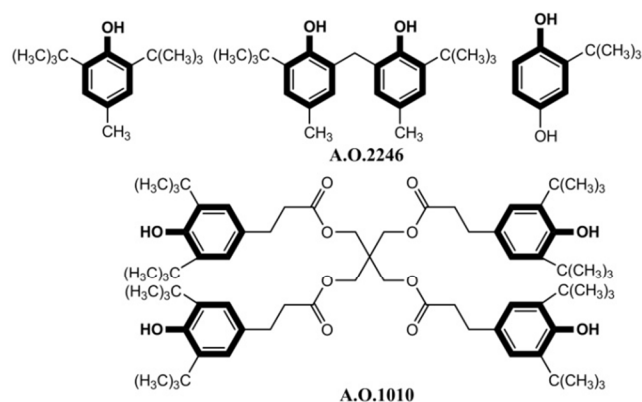


Figure 1. Selected examples of phenolic antioxidants.

The synthesis of bisphenolic antioxidants has been performed in the presence of different homogeneous and heterogeneous catalysts such as H_2SO_4 ,¹⁴⁻¹⁶ HCl ,¹⁷ CF_3COOH ,¹⁸ heteropolyacid,^{19, 20} zeolites,²¹ silica sulfuric acid,²² $[\text{Ir}(\text{COD})\text{Cl}]_2\text{-SnCl}_4$,²³ AuCl_3 or $\text{AuCl}_3/\text{AgOTf}$,²⁴ $\text{Cu}(\text{OTf})_2$,²⁵ FeCl_3 ,²⁶ $\text{Yb}(\text{OTf})_3$,²⁷ $\text{AcBr}/\text{ZnBr}_2/\text{SiO}_2$,²⁸ and multi-walled carbon nanotubes- SO_3H .²⁹ However, the usages of these homogeneous catalytic systems are not suitable for practical application because they are toxic, corrosive, non-reusable, and non-recoverable. Other disadvantages of homogeneous catalyst include environmental pollution, difficulty in work-up, and generally they need additional neutralization stages. Therefore, the development a novel heterogeneous catalyst system with good reusability and appropriate catalytic activity is an important challenge in the synthesis of bisphenolic antioxidants. In spite of their potential applications for the heterogeneous catalysts, many research papers for synthesis of bisphenolic antioxidants have reported some problems such as; long reaction times, excess amount of catalyst, use of toxic organic solvent, and non-reusable catalytic systems for the preparation of bisphenolic antioxidants.

Graphene a single two-dimensional (2D) large of carbon atoms, has attracted much attention in recent years.³⁰ Graphene and graphene oxide (GO) have fascinating physical, optical, and mechanical properties.^{31, 32} Moreover, graphene and GO have large specific surface area, high surface-to-volume ratio,³³ and chemical stability. Due to the large specific surface area, and chemical and thermal stability of GO and graphene, it were employed in chemical process and organic synthesis as support. Solid acid have shown great potential to replace traditional homogeneous liquid acid as environmentally safe acid catalysts.³⁴⁻³⁶ Among them, sulfonated based carbon materials are useful as solid acid catalysts in organic transformations.³⁷⁻⁴¹ A series of sulfonated carbon catalysts was prepared through direct carbonization of raw materials (sugar, cellulose)^{42, 43} followed by the sulfonation of resulted carbons. These catalysts possessed low surface area ($\sim 2 \text{ m}^2/\text{g}$) and do not swell and exhibited much better thermal stability.³⁷ The sulfonated activated carbon (AC) has high specific surface area, and low cost. An early experimental result from Hara's group showed that heating AC in H_2SO_4 and concentrated H_2SO_4 only produced AC with 0.15 mmol.g^{-1} and 0.44 mmol.g^{-1} SO_3H groups density respectively. This fact (low density of SO_3H groups) attributed to the chemical inertness of AC.⁴⁴ Recently, Alamdari, et al. prepared sulfonated single and

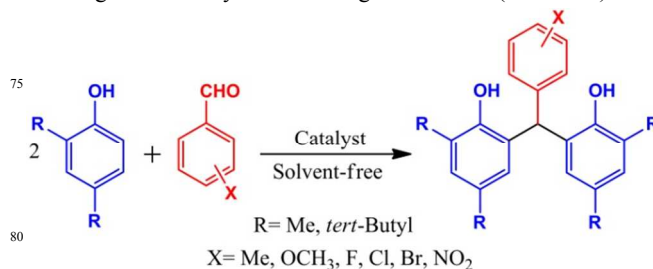
multi walled carbon nanotubes via chemical process. But, the high cost, and hard synthesis of carbon nanotubes are disadvantages of the reported papers.^{40, 41}

Because of prominent properties of graphene and GO such as low cost, easy synthesis, high specific surface area, and chemical and thermal stability, they can be enhanced catalytic activity and provided an excellent support for the heterogeneous catalysts in organic synthesis. Due to the interesting properties of GO and reduced graphene oxide (RGO) as support for the preparation of heterogeneous catalytic systems, we decide to plan three types of catalysts based on GO and RGO nanosheets with various synthetic routes for anchored sulfonated groups on the surface of GO and RGO nanosheets. Furthermore, we hope to compare the activities of three types of prepared catalysts in the synthesis of bisphenolic antioxidants as the same organic reaction from the view of efficiency of catalytic activity, turnover frequency (TOF), power of acidity, the ability of reusability, and time of the reaction performance.

In continuation of our interest towards carbon based materials^{47, 48} and green methodologies,⁴⁹⁻⁵¹ we report the use of RGO and GO as support for attachment of sulfonated groups. The ability of these heterogeneous catalysts were investigated in the synthesis of 6,6'-(arylmethylene)bis(2,4-dialkylphenol) antioxidants from 2,4-dialkylphenol and aromatic aldehydes in atomic economic conditions.

Results and discussion

The synthesis of 6,6'-(arylmethylene)bis(2,4-dialkylphenol) antioxidants is depicted in Scheme 1. Initially, three types of catalysts according to experimental section were prepared and it investigated in the synthesis of target molecules (Scheme 1).

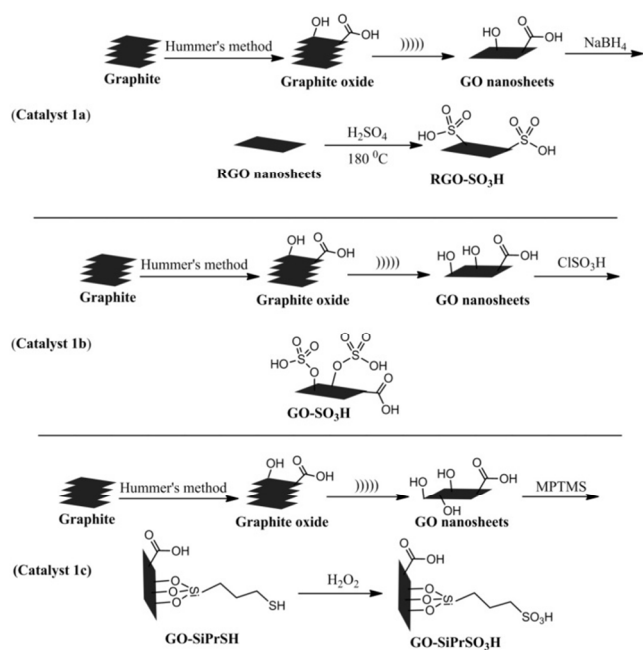


Scheme 1. Synthesis of bisphenolic antioxidants.

Preparation of the catalysts

To start our investigation, it was proceeded to prepare three different solid acids based graphene nanosheets including RGO- SO_3H (**1a**), GO- SO_3H (**1b**), and GO-SiPr SO_3H (**1c**). Schematic illustrations of prepared catalysts are shown in Scheme 2. This

allowed us to have several solid acid catalysts with different types of sulfonated groups anchored on graphene support and various hydrophobic properties for preparation of heterogeneous catalysts. The catalysts **1a**, **1b**, and **1c** were achieved in four, three, and four steps respectively as described in Scheme 2. The GO is the same precursor for the preparation of three types of catalysts. First, natural graphite which is commercially available was converted to graphite oxide using sodium nitrate, H₂SO₄, and potassium permanganate.⁵² This step introduced oxygen containing groups for example epoxy, hydroxyl, and carboxylic acid groups on the surface of graphite. After that, the graphite oxide was sonicated (75 w) for 15 min to produce GO nanosheets. For the preparation of catalyst **1a**, the GO was treated with NaBH₄ as reducing agent and H₂SO₄ (100 %) to afford the RGO-SO₃H. Also, the catalyst **1b** was synthesized from GO nanosheets by treatment of chlorosulfonic acid as a sulfonating agent to obtain GO-SO₃H. In continuous, the catalyst **1c** was obtained in four steps from the reaction of GO nanosheets with mercaptopropyl trimethoxysilane (MPTMS) to afford GO-SiPrSH. Then, the GO-SiPrSH was oxidized to sulfonic acid by H₂O₂ (30 %) to prepare GO-SiPrSO₃H.



Scheme 2. Synthetic routes for the preparation of the three types catalysts.

25 *Characterization of the catalysts*

The prepared catalysts **1a**, **1b**, and **1c** were characterized by some microscopic and spectroscopic techniques including FE-SEM,

TEM, AFM, FT-IR, Raman spectroscopy, XRD, and back acid-base titration.

The FE-SEM images of GO, RGO-SO₃H, GO-SO₃H, and GO-SiPrSO₃H are shown in Figure 2. Different morphologies were observed for pristine GO nanosheets and three types of the prepared catalysts. As shown in Figure 2a, it was found that GO nanosheets consists of randomly aggregated, crumpled, transparent, and flake-like sheets which also observed with wrinkles and folds on the surface of GO nanosheets. The shown morphologies in this Figure exhibit that the large two-dimensional GO nanosheets with layered structures reveal face to face stacking of sheets. The observed morphology in Figure 2b shows significant difference between GO nanosheets and RGO-SO₃H. The RGO-SO₃H shows similar two-dimensional features with foreign matter that it was covered surface of GO nanosheets after reduction and sulfonation, respectively. Figure 2c, shows FE-SEM image of the GO-SO₃H from the treatment of chlorosulfonic acid as a sulfonated agent with GO nanosheets. Comparison of the pristine GO with the GO-SO₃H images was found that it was covered by a layer foreign matter resulting in thickness GO nanosheets flake-like sheets and denser network of two-dimensional GO. As can be shown in Figure 2d, the structure of catalyst **1c** is still flake-like sheets after treatment of MPTMS and H₂O₂. Also, it seems that the morphology of GO-SiPrSO₃H is different in compared with the pristine GO nanosheets due to the functionalization process (Figure 2, image d vs a).

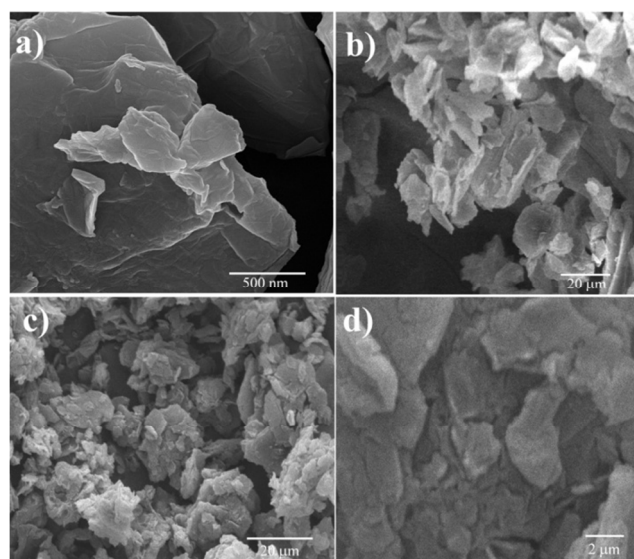


Figure 2. FE-SEM images of a) GO nanosheets, b) RGO-SO₃H, c) GO-SO₃H, d) GO-SiPrSO₃H.

Figure 3 shows the TEM images of GO and RGO nanosheets. It can be seen that the GO and RGO exhibit a typical exfoliated and two-dimensional nanostructures with a rather and large flat and smooth flake-like morphology with several layers. Also, this

5 Figure reveals that two-dimensional flake-like of pristine graphite is still in GO and RGO nanosheets after Hummer's method.

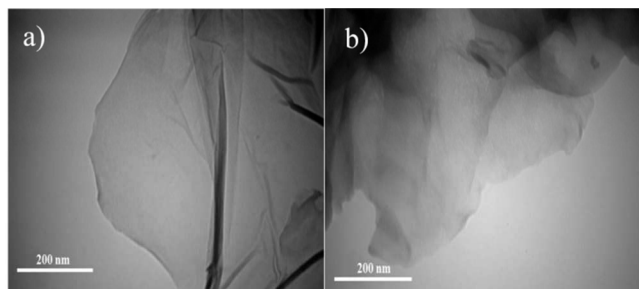


Figure 3. TEM images of a) GO nanosheets b) RGO nanosheets.

10

As shown in Figure 4, the AFM analysis reveals that the measured values of thickness are in the range 0.9-1.5 nm, indicating that exfoliated mono and dilayer graphene oxide was obtained in this study. These graphene oxide layers should be

15 mostly monolayered, although these amount are somewhat larger than the interlayer spacing (0.78 nm) of the parent GO. The sheets are a little more 'bumpy' than predicted, which is possibly due to the existence of abundant functional groups, such as carboxylic, epoxy, and hydroxyl groups, bonded to both sides of

20 the graphene oxide sheets, which disrupts the original conjugation and introduces lattice defects to result in folds and distortions on the sheets.

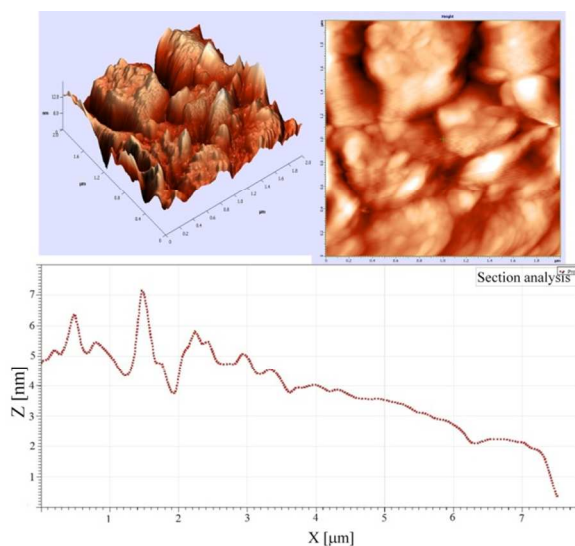


Figure 4. AFM image of GO nanosheets.

25 Figure 5, shows the FT-IR spectra of pristine graphite, GO, RGO, RGO-SO₃H, GO-SO₃H, GO-SiPrSH, and GO-SiPrSO₃H. FT-IR is a tool mainly used to identify the presence or absence of functional groups in chemistry. The high symmetry introduced to pristine graphite generates very weak infrared peaks due to the

30 weak difference of charge states and very small induced electric dipole. The peak related to C=C double bonds at 1573 cm⁻¹ is not sharp in the spectrum of graphite (Figure 5a). The process of Hummer's method and sonication breaks the symmetry of graphite. The FT-IR spectrum of GO was shown in Figure 5b.

35 The peak at approximately 1580 cm⁻¹ is attributed to C=C double bonds. This peak is sharper than graphite due to the un-symmetry of GO. This spectrum shows peaks at 1064, 1719, and 3394 cm⁻¹ which could be assigned to C-O, carbonyl, and hydroxyl stretching mode of functional groups attachment to GO

40 respectively. The chemical reduction of GO with NaBH₄ produce RGO that the spectrum of RGO is shown in Figure 5c. This spectrum shows that the peaks of the hydroxyl and carbonyl groups were disappeared due to the used NaBH₄ as reducing agent. The peak at 3423 cm⁻¹ is related to presence of water on

45 KBr pellets. Also, the presence of the peak at 1566 cm⁻¹ show that after chemical reduction at 100 °C for 24 h, the RGO is still flake-like sheets. Figure 5d and 5e show the FT-IR spectra of RGO-SO₃H and GO-SO₃H. These spectra show peaks related to C-O, carbonyl, and hydroxyl groups at about 1020, 1725, and

50 3400 cm⁻¹ respectively. The FT-IR data confirmed that the functionalization of GO with H₂SO₄ and chlorosulfonic acids occurred to afford RGO-SO₃H and GO-SO₃H. In addition, the FT-IR spectra of GO-SiPrSH and GO-SiPrSO₃H are shown in Figure 5f and 5g respectively. The FT-IR spectra in Figure 5f and

55 5g indicate that the functionalization of MPTMS on the GO was happened due to the presence of the peaks at about 2924 cm⁻¹ related to C-H (*sp*³) stretching mode. After oxidation process with H₂O₂ (30%), these peaks were still on the surface of GO and the peak at 3432 cm⁻¹ was clearly appeared related to -OH of

60 sulfonated groups.

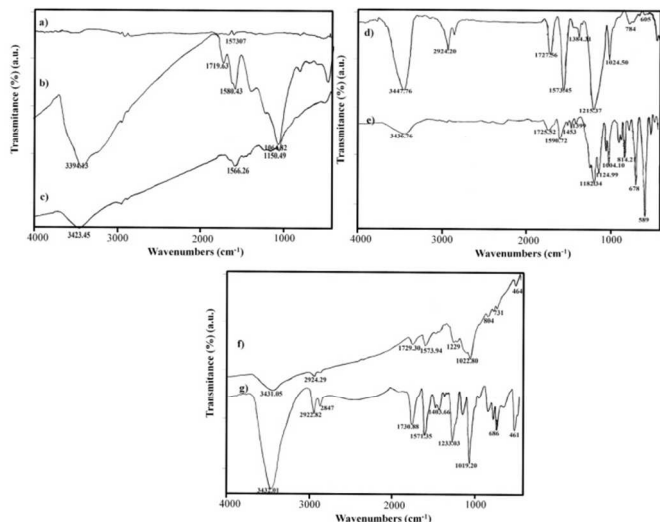


Figure 5. FT-IR spectra of a) Graphite b) GO c) RGO d) RGO-SO₃H e) GO-SO₃H f) GO-SiPrSH g) GO-SiPrSO₃H.

Figure 6 shows XRD patterns of graphite, GO, RGO, and RGO-SO₃H. The XRD pattern of graphite (Figure 6a) shows a strong peak at approximately $2\theta = 26.5^\circ$ corresponding to the feature of graphite. After to do Hummer's method, the peak at about $2\theta = 26.5^\circ$ was broad peak and the peak at $2\theta = 12^\circ$ was appeared. The interlayer spacing (*d*-spacing) of GO was calculated 0.78 nm which revealed the introduction of oxygen species on the graphene network sheets (Figure 6b).⁵³ After chemical reduction of exfoliated GO with NaBH₄, the diffraction peak of GO at $2\theta = 12^\circ$ was disappeared and a broad peak at centered $2\theta = 24^\circ$ was observed, indicating the fully reduction and exfoliation of GO and the production of RGO nanosheets.⁵⁴ As shown in Figure 6c, in the RGO nanosheets was rather broad peak and significantly different from that observed for pristine graphite. Figure 6d shows XRD pattern of RGO-SO₃H after hydrothermal sulfonation. The XRD pattern (Figure 6d) has very similar peaks to RGO suggesting their similar crystal structure of the graphene layers.

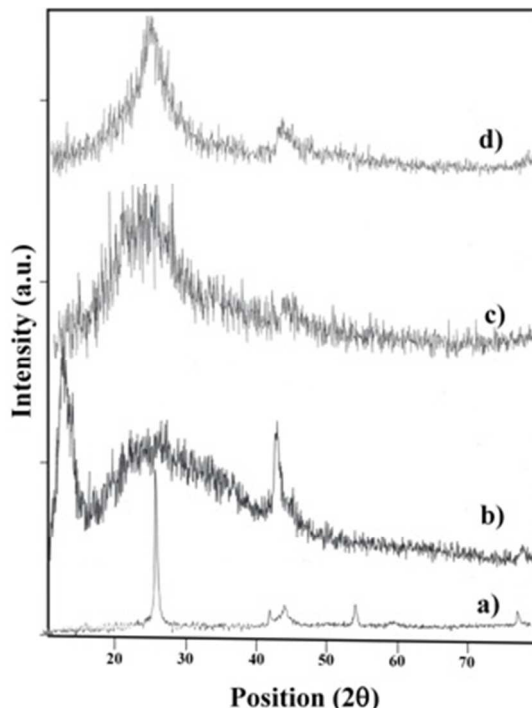


Figure 6. XRD patterns of a) Graphite b) GO c) RGO d) RGO-SO₃H.

Typical Raman spectrum of GO nanosheet is shown in Figure 7. The D and G band were appeared at about 1347 cm⁻¹ and 1593 cm⁻¹ respectively. The G-band arises from the stretching of the C-C bond in graphitic materials, and is related to *sp*² carbon systems. The D-band is caused by disordered structure of graphene. The presence of disorder in *sp*²-hybridized carbon systems results in resonance Raman spectra. The other Raman bands were observed at 2717 cm⁻¹ (2D band), and 2931 cm⁻¹ (D+G-band).⁵⁵ Combined with the G-band, this spectrum is a Raman signature of graphitic *sp*² materials, and 2D-band is a second-order two-phonon process and exhibits a strong frequency dependence on the excitation energy.

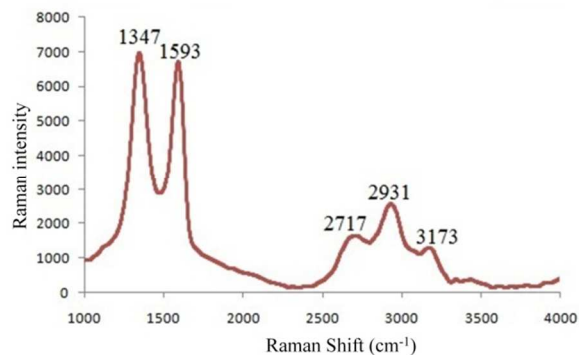


Figure 7. Raman spectrum of GO.

40

Acidity of the catalysts (1a, 1b, 1c)

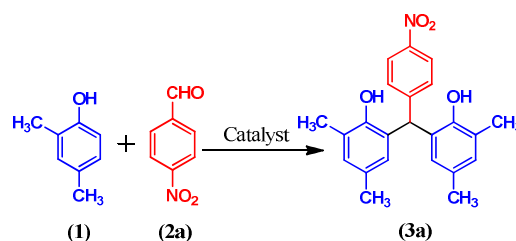
The total amount of the sulfonated groups was measured in the three types of the catalysts using back acid-base titration. The back acid-base titration showed that the density of sulfonated groups anchored on graphene layers for catalysts **1a**, **1b**, and **1c** were 2.15, 1.2, and 0.85 mmol. g⁻¹, respectively.

Catalytic activity of prepared catalysts in the synthesis of bisphenolic antioxidants under solvent free conditions

The prepared three types of the catalysts were employed in the synthesis of 6,6'-(arylmethylene)bis(2,4-dialkylphenol) antioxidants. Initially, the reaction parameters were optimized in the reaction of 2,4-dimethylphenol (**1**) and 4-nitrobenzaldehyde (**2a**) in the presence of catalytic amounts of catalysts **1a**, **1b**, and **1c** as the model reaction. The results are shown in Table 1. The model reaction was optimized in the presence of catalyst **1a** (Table 1, entries 1-10). To choose the medium of the reaction, the model reaction was performed in various solvents such as EtOH, H₂O, CH₃CN, *n*-hexane, and CHCl₃ and without any solvent (Table 1, entries 1-10). As can be seen, entry 9 gave the best result. Therefore, the solvent free conditions were chosen as the

reaction medium. For optimization of temperature of the reaction, an increase in temperature of the reaction (60 to 110 °C) led to decreased time of the reaction and increased yields of the desired product. At temperature of 100 °C, the yield of the reaction was 92% and it similar at 110 °C (Table 1, entries 9, 10). The model reaction was performed in the different amount of catalyst **1a** (Table 1, entries 10-12). The best result was observed with 40 mg of the catalyst **1a**. The best conditions for catalyst **1a** was resulted; T=100 °C, solvent free, and 40 mg of the catalyst. Furthermore, we examined the model reaction in the presence of different of the catalyst (catalyst **1b**, **1c**) (Table 1, entries 13-28). For two types of the catalysts, solvent free conditions were the best medium of the model reaction (Table 1, entries 17-19 and 25-28). In addition, the temperature of the reaction was investigated for catalyst **1b** and **1c** (Table 1, entries 13, 14 and 20, 21). For catalyst **1b** and **1c**, the 100 °C was the best temperature of the model reaction. Also, the catalytic amounts of catalysts were studied and the best results were 75 and 100 mg for the catalysts **1b** and **1c** respectively (Table 1, entries 15-17 and 22-25).

Table 1. Optimizing the reaction conditions ^a



Entry	Catalyst (mg)	Solvent	T (°C)	Time (min)	Yield (%) ^b
1	1a (40)	EtOH	Reflux	70	60
2	1a (40)	H ₂ O	Reflux	55	70
3	1a (40)	CH ₃ CN	Reflux	90	55
4	1a (40)	<i>n</i> -hexane	Reflux	120	25
5	1a (40)	CHCl ₃	Reflux	120	35
6	1a (40)	Solvent free	60	150	20
7	1a (40)	Solvent free	80	60	55
8	1a (40)	Solvent free	90	50	75
9	1a (40)	Solvent free	100	40	92

10	1a (40)	Solvent free	110	40	92
11	1a (50)	Solvent free	100	40	92
12	1a (30)	Solvent free	100	50	87
13	1b (40)	Solvent free	100	60	65
14	1b (40)	Solvent free	120	60	65
15	1b (60)	Solvent free	100	60	72
16	1b (80)	Solvent free	100	60	75
17	1b (75)	Solvent free	100	60	75
18	1b (75)	EtOH	Reflux	90	65
19	1b (75)	CH ₃ CN	Reflux	90	55
20	1c (40)	Solvent free	100	80	50
21	1c (40)	Solvent free	120	80	55
22	1c (70)	Solvent free	100	75	65
23	1c (90)	Solvent free	100	70	65
24	1c (100)	Solvent free	100	70	68
25	1c (110)	Solvent free	100	75	65
26	1c (100)	H ₂ O	Reflux	100	60
27	1c (100)	EtOH	Reflux	120	60
28	1c (100)	CHCl ₃	Reflux	150	40

a) General reaction conditions: 2,4-dimethylphenol (1) (6 mmol), 4-nitrobenzaldehyde (2a) (2 mmol), solvent (2 mL).

b) Isolated yields.

10

After optimization of the reaction conditions, synthesis of 6,6'-(arylmethylene)bis(2,4-dialkylphenol) antioxidants were performed from the condensation reaction of 2,4-dialkylphenol (1) and different aldehydes (2a-2q) utilizing catalysts 1a, 1b, and 1c under solvent free conditions at 100 °C. As shown in Table 2,

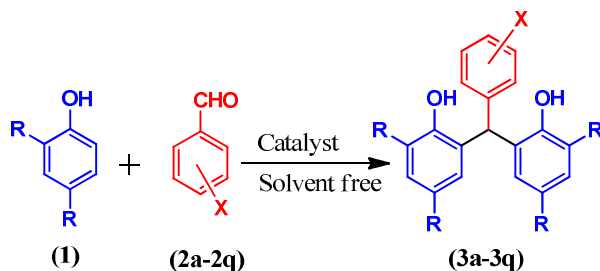
all of the products were synthesized using RGO-SO₃H, GO-SO₃H, and GO-SiPrSO₃H. As shown in Table 2, aromatic aldehydes with electron-withdrawing groups on ortho or para position accelerate the time of the reaction and improved yield of desired products compared with the electron-donating groups on ortho or para position. Also, it was observed that the catalyst 1a was better than other catalysts. In the catalyst 1a, the total density of SO₃H groups is higher than other catalysts.

20

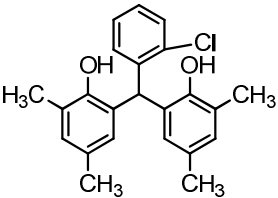
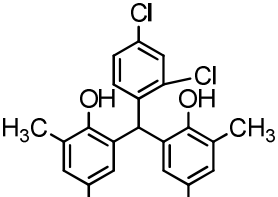
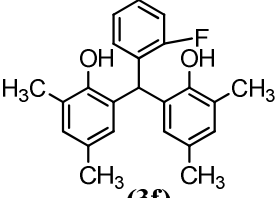
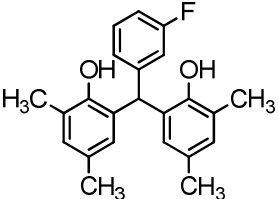
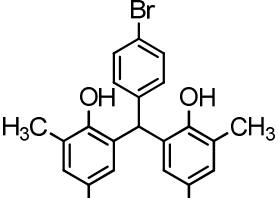
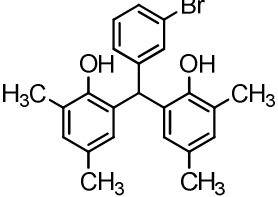
Cite this: DOI: 10.1039/c0xx00000x

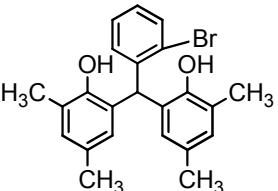
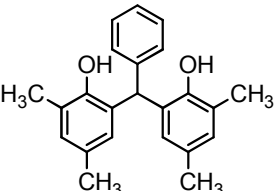
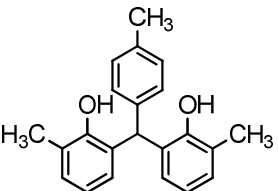
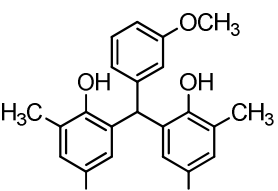
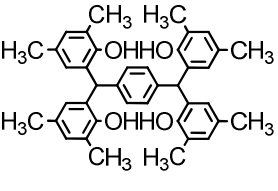
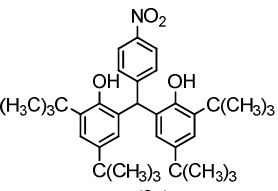
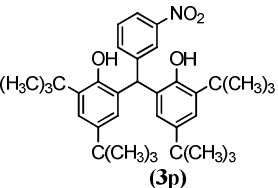
www.rsc.org/xxxxxx

PAPER

Table 2. Synthesis of 6,6'-(arylmethylene)bis(2,4-dialkylphenol) antioxidants ^a

Entry	R	X	Product	Catalyst 1a			Catalyst 1b			Catalyst 1c		
				(RGO-SO ₃ H)			(GO-SO ₃ H)			(GO-SiPrSO ₃ H)		
				Time (min)	Yield (%) ^b	TOF (h ⁻¹)	Time (min)	Yield (%) ^b	TOF (h ⁻¹)	Time (min)	Yield (%) ^b	TOF (h ⁻¹)
1	CH ₃	4-NO ₂	<p style="text-align: center;">(3a)</p>	40	92	16.2	60	75	8.3	70	68	6.9
2	CH ₃	3-NO ₂	<p style="text-align: center;">(3b)</p>	45	93	14.4	75	81	7.2	90	74	5.8
3	CH ₃	4-Cl	<p style="text-align: center;">(3c)</p>	30	90	20.9	35	88	16.8	60	82	9.6

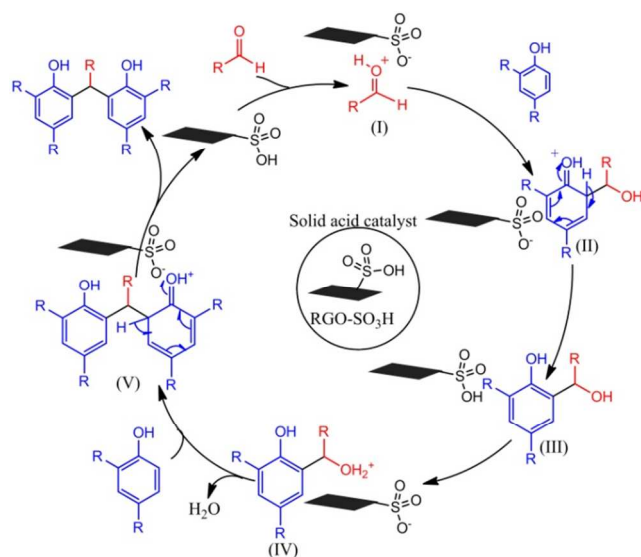
4	CH ₃	2-Cl		30	94	21.8	45	76	18.7	80	73	6.4
			(3d)									
5	CH ₃	2,4-Cl		25	89	24.6	30	85	18.9	35	85	17.2
			(3e)									
6	CH ₃	2-F		40	82	14.4	50	76	10.2	90	65	5.1
			(3f)									
7	CH ₃	3-F		30	90	20.9	45	75	11.1	70	65	6.6
			(3g)									
8	CH ₃	4-Br		20	95	33.5	25	80	21.2	40	80	14.3
			(3h)									
9	CH ₃	3-Br		30	88	20.5	40	76	12.8	60	58	6.8
			(3i)									

10	CH ₃	2-Br		15	89	41.4	25	86	22.8	25	82	23.0
			(3j)									
11	CH ₃	H		60	80	9.3	100	76	5.1	120	79	4.6
			(3k)									
12	CH ₃	4-CH ₃		60	81	9.4	120	79	4.4	150	68	3.2
			(3l)									
13	CH ₃	3-OCH ₃		50	78	10.9	100	80	5.3	130	67	3.6
			(3m)									
14 ^c	CH ₃	4-CHO		30	82	19.1	35	79	15.1	40	79	14.1
			(3n)									
15	<i>tert</i> -butyl	4-NO ₂		60	89	10.3	75	85	7.5	100	68	4.8
			(3o)									
16	<i>tert</i> -butyl	3-NO ₂		50	90	12.6	80	80	6.7	110	71	4.6
			(3p)									

17^d CH₃ CH₂O 10 96 69.7 15 91 40.4 30 79 18.6

- a) General reaction conditions: 2,4-dialkylphenol (**1**) (6 mmol), aldehyde (2a-2q) (2 mmol), solvent free, T= 100 °C, catalysts 1a= 40 mg, 1b= 75 mg, 1c= 100 mg.
 b) Isolated yields.
 c) Reaction conditions: 2,4-dimethylphenol (12 mmol), terphthaldehyde (2n) (2 mmol).
 d) Reaction conditions: 2,4-dimethylphenol (4 mmol), formaldehyde (2q) (2 mmol).

The proposed reaction mechanism for solid acid catalysts based on graphene nanosheets catalyzed synthesis of 6,6'-(arylmethylene)bis(2,4-dialkylphenol) antioxidants using 2,4-dialkylphenol and aromatic aldehydes are shown in Scheme 3. The reaction proceeds via a series of protonic shifts from solid acid catalysts to the substrates. First, the aromatic aldehydes are activated by protonation with solid acid catalysts to give species (I). Nucleophilic attack of 2,4-dialkylphenol on (I) affords species (II) and (III) which in turn is activated by solid acid catalysts to afford species (IV). Nucleophilic attack of second molecule of 2,4-dialkylphenol to species (IV), gives (V) which is subsequently converted to 6,6'-(arylmethylene)bis(2,4-dialkylphenol) antioxidants and releases solid acid catalysts for the next catalytic runs.



Scheme 3. The proposed reaction mechanism.

The reusability and stability of the catalyst 1a

For practical application of solid acid catalysts in industrial, the life time and stability of the RGO-SO₃H are very important factors. The homogeneous acidic catalysts cannot recover even one time, in contrast with the solid acid catalysts such as RGO-SO₃H. The reusability of the catalyst **1a** was studied in the multiple sequential reaction of 2,4-dimethylphenol (**1**) and 4-bromobenzaldehyde (**2h**). The catalyst was consecutively recovered for eight cycles without significant loss of its catalytic activity (Figure 8). At the end of each reaction, the solid acid catalyst was isolated by simple filtration under reduced pressure, washed exhaustively with acetone, *n*-hexane, and ethanol, and dried at 100 °C for 24 h before being used with fresh 2,4-dimethylphenol and 4-bromobenzaldehyde. The catalyst can be reused for eight runs without any treatment in its catalytic activity.

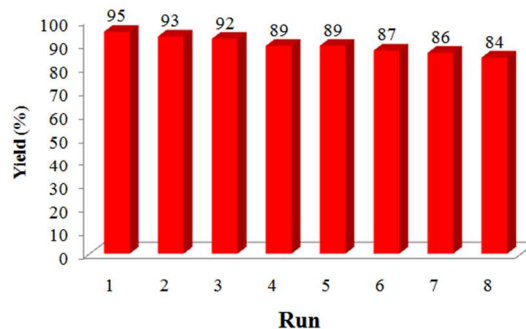


Figure 8. The reusability of the catalyst 1a in the synthesis of (**3h**).

Conclusions

In conclusions, in this study, three types of the solid acid catalysts based reduced graphene oxide or graphene oxide nanosheets were prepared and were investigated in the synthesis of 6,6'-(arylmethylene)bis(2,4-dialkylphenol) antioxidants under solvent free conditions. The total density of SO₃H groups on the surface of solid acid catalysts for RGO-SO₃H, GO-SO₃H, and GO-

20

SiPrSO₃H were 2.15, 1.20, and 0.85 mmol. g⁻¹. The RGO-SO₃H relative to another two types of the prepared catalysts is more reactive and stable in the synthesis of bisphenolic antioxidants because of the high acidity. For the first time, we disclosed a highly efficient method for the preparation of 6,6'-(arylmethylene)bis(2,4-dialkylphenol) antioxidants from 2,4-dialkylphenol and aldehydes under atomic economic and solvent free conditions.

Experimental

Materials and apparatus

The chemicals used in this work were purchased from Fluka and Merck chemical companies and used without purification. IR spectra were obtained as KBr pellets in the range of 400-4000 cm⁻¹ on a Perkin-Elmer 781 spectrophotometer and on an impact 400 Nicolet FT-IR spectrophotometer. ¹H NMR and ¹³C NMR spectra were recorded in DMSO-(d₆) solvent on a Bruker DRX-400 MHz spectrometer using tetramethyl silane as an internal standard. XRD patterns were recorded by an X'PertPro (Philips) instrument with 1.54° A wavelengths of X-ray beam and Cu anode material, at a scanning speed of 2°/min from 10° to 80° (2θ). The elemental analyses (C, H, N) were obtained from a Carlo ERBA Model EA 1108 analyzer. The Raman spectra were recorded with an Almega Thermo Nicolet Dispersive Raman spectrometer excited at 532 nm. Scanning electron microscopy (SEM) of prepared catalysts was taken on a FE-SEM Hitachi S4160 instrument. Transmission electron microscopy (TEM) was recorded with a Zeiss-EM10C with an acceleration voltage of 80 kV. The atomic force microscopy (AFM) of GO nanosheets was measured using a scanning probe microscope (SPM-9600, shimadzu). Melting points was obtained with a Yanagimoto micro melting point apparatus and are uncorrected. The purity determination of the substrates and reaction monitoring were accomplished by TLC on silica-gel polygram SILG/UV 254 plates (from Merck Company).

Typical procedure for the preparation of GO nanosheets

GO nanosheets were synthesized using graphite powders by a modified Hummer's method⁵². Typically, 5.0 g of natural graphite powder and 2.5 g of sodium nitrate were mixed with 115 mL of sulfuric acid (98%) in a 1000 mL round-bottom flask equipped with a magnetic stirrer and condenser place in an ice

bath. The obtained solution was stirred and slowly added 15.0 g of potassium permanganate, the stirring was continued for 2 h. The mixture solution was transferred to a 35 °C water bath and stirred for 30 min. After this step, 230 mL of deionized water was slowly added into the solution and the solution temperature monitored was about 98 °C and stirred for 15 min. Then, 700 mL of deionized water and 50 mL of H₂O₂ (30%) was sequentially added to the mixture solution to terminate the reaction. The resulting materials was filtered and washed with 5% HCl solution followed by distilled water for several times. The solution was filtered under reduced pressure by vacuum pump over sinter-glass (G4). The graphite oxide powder was obtained after drying in vacuum at 60 °C for 12 h. The graphite oxide was dispersed in distilled water to make concentration of 0.5 mg/mL, and exfoliated by ultrasonication (75 w) for 30 min to generate GO nanosheets, followed by centrifugation at 3500 rpm for 30 min to remove unexfoliated graphite oxide.

Typical procedure for the preparation of sulfonated reduced graphene oxide nanosheets (1a)

For preparation of catalyst **1a**, first, reduced graphene oxide (RGO) was synthesized by the chemical reduction of GO using NaBH₄ as a reducing agent. In a 1000 mL round-bottom flask, 1.0 g of the GO dispersion was added into deionized water (700 mL), followed by sonication (40 w) for 15 min. Then, 2.4 g of NaBH₄ was added into the round-bottom flask, heating at 100 °C for 24 h. After this step, the resulted product was washed with water several times and filtered under reduced pressure by vacuum pump over sinter glass (G4) and centrifugation at 3500 rpm for 15 min to obtain RGO nanosheetss. Sulfonated reduced graphene oxide nanosheets (RGO-SO₃H) was prepared from the hydrothermal sulfonation of RGO using H₂SO₄ (100 %) at 180 °C. 1.0 g of RGO was added into 50 mL of H₂SO₄. After sonication (40 w) for 15 min, the mixture was transferred into a round-bottom flask under nitrogen atmosphere and stirring to heat at 180 °C for 24 h. Then, the prepared catalyst **1a** was washed with a large amount of deionized water and drying at 80 °C for 12 h. Finally RGO-SO₃H was obtained and checked in the synthesis of bisphenolic antioxidants.

Typical procedure for the preparation of sulfonic acid graphene oxide nanosheets (1b)

For preparation of catalyst **1b**, in a typical experiment, GO (0.5 g), dichloromethane (4 mL), and chlorosulfonic acid (1.5 mL) were added to round-bottom flask 25 mL and stirred at room

temperature for 24 h under nitrogen atmosphere. After this step, the resulted catalyst was thoroughly washed with deionized water and ethanol several times and filtered under reduced pressure over sinter glass (G4). The solid acid **1b** was dried at 90 °C for 24 h and finally the GO-SO₃H was obtained and used in the synthesis of bisphenolic antioxidants.

Typical procedure for the preparation of the sulfonated propylsilane graphene oxide nanosheets (1c)

For preparation of catalyst **1c**, the GO was functionalized with mercaptopropyl trimethoxysilane (MPTMS) as the organic precursor for the preparation of sulfonated propylsilane graphene oxide nanosheets (GO-SiPrSO₃H). Firstly, GO (0.5 g), and 3.0 mL of MPTMS was added to 4.0 mL of toluene as a medium reaction and stirred at 110 °C for 24 h. Then, the mercaptopropyl groups of the functionalized GO nanosheets were oxidized to sulfonic acid group using 10 mL of H₂O₂ (30%) as the green oxidizing agent at room temperature for 24 h. The obtained catalyst **1c** was washed with deionized water and ethanol to remove the residual precursor, then, dried at 60 °C for 24 h. The prepared catalyst **1c** was employed in the reaction of 2,4-dialkylphenol and aromatic aldehydes for the synthesis of bisphenolic antioxidants.

General procedure for the preparation of bisphenolic antioxidants catalyzed by catalysts (1a, 1b, 1c) under solvent free conditions

In a 25 mL round-bottom flask equipped with a magnetic bar and condenser, a mixture of 2,4-dialkylphenol (6 mmol), aromatic aldehyde (2 mmol) and RGO-SO₃H (**1a**) (40 mg) was heated at 100 °C under solvent free conditions for the appropriate time according to Table 2. The progress of the reaction was monitored by thin layer chromatography (TLC) (n-hexane: ethyl acetate 10:4). At the end of the reaction, the mixture was cooled to room temperature and 15 mL of acetone (3×5 mL) was added. The RGO-SO₃H was filtered under reduced pressure using vacuum pump over sinter glass (G4). The solution was recovered by evaporation on a rotary evaporator. After that, the solid materials were washed with n-hexane (5 mL) and deionized water, successively, to afford pure products. The desired products were kept in an oven at 80 °C for 12 h. In addition, the prepared catalysts **1b**, and **1c** were investigated in the synthesis of bisphenolic antioxidants. The amount of the catalyst **1b**, and **1c**

were 75, and 100 mg respectively and appropriate time were added to Table 2.

Acidity of the prepared catalysts

The density of sulfonated group on RGO, and GO was calculated by back acid-base titration. First, 100 mg of RGO-SO₃H was ultrasonicated in a water bath for 10 min under nitrogen atmosphere to degas CO₂. Next 10 mL of NaOH 0.098 N was added and the mixture stirred for 2 h at room temperature. Subsequently, the mixture was filtered through sintered glass (G-4) and washed several times with deionized water. The filtrate was then titrated with HCl 0.1 N until reaching the neutral point as monitored by phenolphthalein as indicator. The volume required to reach the neutral point was subtracted from the initial volume of NaOH used to obtain the volume of NaOH which has reacted with sulfonated group on RGO or GO. The back acid-base titration for GO was carried out and the results calculated in the acidity of catalyst **1a** and **1b**. The measurement was repeated three times for each catalyst and the average calculated (Equation 1).

(Equation 1)

$$\text{NaOH (mmol reacted with SO}_3\text{H)} = \text{NaOH (primary mmol)} - \text{NaOH (mmol unreacted with SO}_3\text{H)}$$

Regeneration of the catalyst 1a

Recovery and reusability of the heterogeneous catalysts are very important factor in practice and also from economical and industrial viewpoint. Reusability of the RGO-SO₃H was studied in the reaction of 2,4-dimethylphenol and 4-bromobenzaldehyde. At the end of each run, the catalyst was isolated by filtration, washed exhaustively with acetone, n-hexane, and ethanol, then dried at 100 °C for 12 h before being used with fresh 2,4-dimethylphenol and 4-bromobenzaldehyde. The catalyst **1a** can be reused eight cycles without any reduction in its catalytic activity.

Spectroscopic and physical data

6,6'-((4-nitrophenyl)methylene)bis(2,4-dimethylphenol) (Table 2, Compound **3a**): mp: 136-138 °C; IR (KBr): ν (cm⁻¹) 3482, 3249, 2958, 1599, 1522, 1475, 1349, 1292, 1113, 879. ¹H-NMR (400 MHz, DMSO-d₆) δ (ppm): 1.95 (6H, s, Me), 2.47 (6H, s, Me), 6.22 (1H, s, Ar₃CH), 6.26 (2H, s, OH), 6.75 (2H, s, 3-H DMP), 7.21 (2H, d, $J=8$ Hz, 2,6-H aldehyde), 8.09 (2H, s, 5-H DMP), 8.11 (2H, d, $J=8$ Hz, 3,5-H aldehyde). Anal. Calcd for C₂₃H₂₃NO₄: C, 73.19; H, 6.14; N, 3.71%. Found: C, 73.06; H, 6.12; N, 3.70%.

6,6'-((3-nitrophenyl)methylene)bis(2,4-dimethylphenol) (Table 2, Compound **3b**): mp: 141-143 °C; IR (KBr): ν (cm⁻¹) 3433, 3082, 2916, 1606, 1525, 1481, 1347, 1217, 1096, 861. ¹H-NMR (400 MHz, DMSO-d₆) δ (ppm): 1.91 (6H, s, Me), 2.46 (6H, s, Me), 6.24 (1H, s, Ar₃CH), 6.28 (2H, s, OH), 6.57 (2H, s, 3-H DMP), 6.75 (1H, d, $J=7.8$ Hz, 5-H aldehyde), 7.43 (1H, d, 6-H aldehyde), 7.53 (2H, d, $J=7.8$ Hz, 2,4-H aldehyde), 7.73 (2H, s, 5-H DMP). Anal. Calcd for C₂₃H₂₃NO₄: C, 73.19; H, 6.14; N, 3.71%. Found: C, 73.21; H, 7.05; N, 3.67%.

6,6'-((4-chlorophenyl)methylene)bis(2,4-dimethylphenol) (Table 2, Compound **3c**): mp: 158-160 °C; IR (KBr): ν (cm⁻¹) 3498, 3467, 3018, 2918, 1587, 1472, 1381, 1254, 1183, 1048, 862. ¹H-NMR (400 MHz, DMSO-d₆) δ (ppm): 2.03 (6H, s, Me), 2.08 (6H, s, Me), 6.10 (1H, s, Ar₃CH), 6.26 (2H, s, OH), 6.71 (2H, s, 3-H DMP), 6.96 (2H, d, $J=7.9$ Hz, 2,6-H aldehyde), 7.28 (2H, s, 5-H DMP), 7.97 (2H, d, $J=7.9$ Hz, 3,5-H aldehyde). Anal. Calcd for C₂₃H₂₃ClO₂: C, 75.30; H, 6.32%. Found: C, 75.19; H, 6.29%.

6,6'-((2-chlorophenyl)methylene)bis(2,4-dimethylphenol) (Table 2, Compound **3d**): mp: 191-193 °C; IR (KBr): ν (cm⁻¹) 3482, 2918, 1600, 1598, 1474, 1331, 1291, 1190, 1037, 866. ¹H-NMR (400 MHz, DMSO-d₆) δ (ppm): 1.93 (6H, s, Me), 2.08 (6H, s, Me), 6.19 (2H, s, OH), 6.40 (1H, s, Ar₃CH), 6.71 (2H, s, 3-H DMP), 6.83 (1H, t, $J=8$ Hz, 4-H aldehyde), 7.18 (2H, s, 5-H DMP), 7.35 (1H, d, $J=7.7$ Hz, 6-H aldehyde), 7.96 (2H, d, 3,5-H aldehyde). Anal. Calcd for C₂₃H₂₃ClO₂: C, 75.30; H, 6.32%. Found: C, 75.29; H, 6.34%.

6,6'-((2,4-dichlorophenyl)methylene)bis(2,4-dimethylphenol) (Table 2, Compound **3e**): mp: 183-185 °C; IR (KBr): ν (cm⁻¹) 3500, 3466, 3022, 2917, 1602, 1481, 1405, 1252, 1184, 1138, 847. ¹H-NMR (400 MHz, DMSO-d₆) δ (ppm): 1.92 (6H, s, Me), 2.08 (6H, s, Me), 6.17 (2H, s, OH), 6.33 (1H, s, Ar₃CH), 6.73 (2H, s, 3-H DMP), 7.80 (2H, s, 5-H DMP), 7.29 (1H, d, $J=8$ Hz, 6-H aldehyde), 7.50 (1H, d, $J=8$ Hz, 5-H aldehyde), 8.01 (1H, s, 2H aldehyde). Anal. Calcd for C₂₃H₂₂Cl₂O₂: C, 68.83; H, 5.53%. Found: C, 68.64; H, 5.49%.

6,6'-((2-fluorophenyl)methylene)bis(2,4-dimethylphenol) (Table 2, Compound **3f**): mp: 146-148 °C; IR (KBr): ν (cm⁻¹) 3484, 3920, 1584, 1482, 1333, 1290, 1223, 1193, 1140, 866. ¹H-NMR (400 MHz, DMSO-d₆) δ (ppm): 1.95 (6H, s, Me), 2.09 (6H, s, Me), 6.26 (2H, s, OH), 6.35 (1H, s, Ar₃CH), 6.72 (2H, s, 3-H DMP), 6.72 (1H, t, $J=7.8$ Hz, 4-H aldehyde), 7.06 (2H, s, 5-H

DMP), 7.20 (1H, d, $J=8$ Hz, 6-H aldehyde), 7.98 (2H, d, t, 3,5-H aldehyde). ¹³C-NMR (100 MHz, DMSO-d₆) δ (ppm): 17.18, 20.95, 36.84, 115.28, 115.50, 124.44, 127.42, 128.15, 129.80, 130.88, 131.98, 132.13, 150.64, 159.51, and 161.94. Anal. Calcd for C₂₃H₂₃FO₂: C, 78.83; H, 6.62%. Found: C, 78.72; H, 6.61%.

6,6'-((3-fluorophenyl)methylene)bis(2,4-dimethylphenol) (Table 2, Compound **3g**): mp: 94-96 °C; IR (KBr): ν (cm⁻¹) 3335, 3923, 1611, 1586, 1482, 1442, 1385, 1292, 1189, 1142, 783. ¹H-NMR (400 MHz, DMSO-d₆) δ (ppm): 1.95 (6H, s, Me), 2.09 (6H, s, Me), 6.14 (1H, s, Ar₃CH), 6.28 (2H, s, OH), 6.66 (2H, s, 3-H DMP), 6.72 (2H, d, $J=7.9$ Hz, 5,6-H aldehyde), 6.96 (1H, d, $J=7.9$ Hz, 2-H aldehyde), 7.25 (1H, d, $J=7.9$ Hz, 4-H aldehyde), 8.00 (2H, s, 5-H DMP). Anal. Calcd for C₂₃H₂₃FO₂: C, 78.83; H, 6.62%. Found: C, 78.79; H, 6.54%.

6,6'-((4-bromophenyl)methylene)bis(2,4-dimethylphenol) (Table 2, Compound **3h**): mp: >240 °C; IR (KBr): ν (cm⁻¹) 3468, 2917, 1601, 1480, 1401, 1251, 1184, 1138, 1072, 860. ¹H-NMR (400 MHz, DMSO-d₆) δ (ppm): 2.06 (6H, s, Me), 2.08 (6H, s, Me), 6.07 (1H, s, Ar₃CH), 6.25 (2H, s, OH), 6.70 (2H, s, 3-H DMP), 6.88 (2H, d, $J=7.9$ Hz, 2,6-H aldehyde), 7.38 (2H, s, 5-H DMP), 7.96 (2H, d, $J=7.9$ Hz, 3,5-H aldehyde). Anal. Calcd for C₂₃H₂₃BrO₂: C, 67.16; H, 5.64%. Found: C, 67.18; H, 5.61%.

6,6'-((3-bromophenyl)methylene)bis(2,4-dimethylphenol) (Table 2, Compound **3i**): mp: 124-126 °C; IR (KBr): ν (cm⁻¹) 3345, 2922, 1591, 1478, 1383, 1325, 1293, 1188, 1143, 1075, 863. ¹H-NMR (400 MHz, DMSO-d₆) δ (ppm): 2.03 (6H, s, Me), 2.08 (6H, s, Me), 6.10 (1H, s, Ar₃CH), 6.26 (2H, s, OH), 6.72 (2H, s, 3-H DMP), 6.96 (1H, d, $J=8$ Hz, 6-H aldehyde), 7.19 (1H, d, $J=8$ Hz, 5-H aldehyde), 7.21 (1H, $J=7.8$ Hz, 4-H aldehyde), 7.33 (1H, $J=7.8$ Hz, 2-H aldehyde), 8.01 (2H, s, 5-H DMP). ¹³C-NMR (100 MHz, DMSO-d₆) δ (ppm): 17.19, 20.94, 43.50, 121.84, 124.65, 127.57, 128.07, 128.73, 128.98, 129.86, 130.57, 130.94, 131.98, 148.06, and 150.68. Anal. Calcd for C₂₃H₂₃BrO₂: C, 67.16; H, 5.64%. Found: C, 67.08; H, 5.51%.

6,6'-((2-bromophenyl)methylene)bis(2,4-dimethylphenol) (Table 2, Compound **3j**): mp: 188-190 °C; IR (KBr): ν (cm⁻¹) 3484, 2917, 1597, 1566, 1474, 1330, 1189, 1140, 1023, 866, 750. ¹H-NMR (400 MHz, DMSO-d₆) δ (ppm): 1.94 (6H, s, Me), 2.09 (6H, s, Me), 6.18 (2H, s, OH), 6.35 (1H, s, Ar₃CH), 6.72 (2H, s, 3-H DMP), 6.83 (1H, d, $J=8$ Hz, 6-H aldehyde), 7.08 (1H, d, $J=8$ Hz, 4-H aldehyde), 7.21 (1H, d, $J=7.7$ Hz, 3-H aldehyde), 7.53 (1H, t, $J=7.7$ Hz, 5-H aldehyde), 7.97 (2H, s, 5-H DMP). Anal.

Calcd for C₂₃H₂₃BrO₂: C, 67.16; H, 5.64%. Found: C, 67.20; H, 5.59%.

6,6'-((phenyl)methylene)bis(2,4-dimethylphenol) (Table 2, Compound **3k**): mp: 113-115 °C; IR (KBr): ν (cm⁻¹) 3339, 3021, 2920, 1600, 1481, 1447, 1384, 1292, 1186, 1142, 864, 702. ¹H-NMR (400 MHz, DMSO-d₆) δ (ppm): 2.06 (6H, s, Me), 2.08 (6H, s, Me), 6.13 (1H, s, Ar₃CH), 6.29 (2H, s, OH), 6.70 (2H, s, 3-H DMP), 6.97 (2H, t, *J*=8 Hz, 3,5-H aldehyde), 7.11 (1H, t, *J*=8 Hz, 4-H aldehyde), 7.23 (2H, d, *J*=8 Hz, 2,6-H aldehyde), 7.93 (2H, s, 5-H DMP). Anal. Calcd for C₂₃H₂₄O₂: C, 83.10; H, 7.28%. Found: C, 83.14; H, 7.24%.

6,6'-((4-methylphenyl)methylene)bis(2,4-dimethylphenol) (Table 2, Compound **3l**): mp: 168-170 °C; IR (KBr): ν (cm⁻¹) 3501, 2917, 1604, 1476, 1330, 1188, 1139, 1031, 866. ¹H-NMR (400 MHz, DMSO-d₆) δ (ppm): 2.01 (6H, s, Me), 2.07 (6H, s, Me), 2.21 (3H, s, CH₃-aldehyde), 6.06 (1H, s, Ar₃CH), 6.28 (2H, s, OH), 6.68 (2H, s, 3-H DMP), 6.84 (2H, d, *J*=8.1 Hz, 3,5-H aldehyde), 7.01 (2H, s, 5-H DMP), 7.88 (2H, d, *J*=8.1 Hz, 2,6-H aldehyde). ¹³C-NMR (100 MHz, DMSO-d₆) δ (ppm): 17.21, 20.97, 43.26, 124.38, 127.30, 128.18, 128.94, 129.45, 129.58, 131.95, 134.81, 141.78, and 150.69. Anal. Calcd for C₂₄H₂₆O₂: C, 83.20; H, 7.56%. Found: C, 83.14; H, 7.49%.

6,6'-((3-methoxyphenyl)methylene)bis(2,4-dimethylphenol) (Table 2, Compound **3m**): mp: >270 °C; IR (KBr): ν (cm⁻¹) 3453, 2975, 1622, 1505, 1402, 1347, 1230, 1088, 790. ¹H-NMR (400 MHz, DMSO-d₆) δ (ppm): 1.94 (6H, s, Me), 2.08 (6H, s, Me), 3.80 (3H, s, OCH₃), 6.14 (1H, s, Ar₃CH), 6.28 (2H, s, OH), 6.68 (2H, s, 3-H DMP), 6.84 (1H, s, 2-H aldehyde), 6.94 (1H, d, *J*=7.9 Hz, 4-H aldehyde), 7.64 (2H, s, 5-H DMP), 8.12 (2H, m, 5,6-H aldehyde). Anal. Calcd for C₂₄H₂₆O₃: C, 79.53; H, 7.23%. Found: C, 79.58; H, 7.20%.

6,6',6'',6'''-(1,4-phenylenebis(methanetriyl))tetrakis(2,4-dimethylphenol) (Table 2, Compound **3n**): mp: 65-67 °C; IR (KBr): ν (cm⁻¹) 3429, 3012, 2918, 1686, 1602, 1479, 1294, 1208, 1016, 861. ¹H-NMR (400 MHz, DMSO-d₆) δ (ppm): 1.90 (12H, s, Me), 2.10 (12H, s, Me), 6.07 (2H, s, Ar₃CH), 6.25 (4H, s, OH), 6.52 (2H, s, 3-H DMP), 6.61 (4H, m, 2,6-H aldehyde), 6.72 (4H, s, 5-H DMP), 7.77 (2H, m, 3,5-H aldehyde), 7.94 (2H, m, 3,5-H aldehyde). ¹³C-NMR (100 MHz, DMSO-d₆) δ (ppm): 16.41, 17.20, 20.56, 20.95, 43.28, 114.88, 123.88, 124.32, 124.68, 127.30, 127.61, 128.29, 129.19, 129.81, 130.28, 131.58, 132.02,

141.99, 150.66, and 153.50. Anal. Calcd for C₄₀H₄₂O₄: C, 81.88; H, 7.21%. Found: C, 81.82; H, 7.20%.

6,6'-((4-nitrophenyl)methylene)bis(2,4-di-tert-butylphenol) (Table 2, Compound **3o**): mp: 153-155 °C; IR (KBr): ν (cm⁻¹) 3491, 2959, 1690, 1598, 1522, 1474, 1417, 1350, 1188, 116, 862. ¹H-NMR (400 MHz, DMSO-d₆) δ (ppm): 1.05 (18H, s, tert-butyl), 1.33 (18H, s, tert-butyl), 6.28 (1H, s, Ar₃CH), 6.47 (2H, s, OH), 7.13 (2H, s, 3-H DMP), 7.13 (2H, d, *J*=8 Hz, 2,6-H aldehyde), 7.70 (2H, s, 5-H DMP), 8.13 (2H, d, *J*=8 Hz, 3,5-H aldehyde). ¹³C-NMR (100 MHz, DMSO-d₆) δ (ppm): 30.35, 31.70, 34.27, 35.16, 44.12, 121.76, 123.47, 125.08, 130.50, 130.64, 137.52, 141.46, 146.18, 151.02, and 153.25. Anal. Calcd for C₃₅H₄₇NO₄: C, 77.03; H, 8.68; N, 2.57%. Found: C, 77.07; H, 8.61; N, 2.59%.

6,6'-((3-nitrophenyl)methylene)bis(2,4-di-tert-butylphenol) (Table 2, Compound **3p**): mp: 118-120 °C; IR (KBr): ν (cm⁻¹) 3528, 2959, 1530, 1473, 1350, 1186, 1023, 884. ¹H-NMR (400 MHz, DMSO-d₆) δ (ppm): 2.01 (6H, s, Me), 2.06 (6H, s, Me), 6.06 (1H, s, Ar₃CH), 6.29 (2H, s, OH), 6.93 (2H, s, 3-H DMP), 7.16 (1H, d, *J*=8 Hz, 6-H aldehyde), 7.55 (2H, m, 4,5-H aldehyde), 7.64 (2H, s, 5-H DMP), 8.12 (1H, s, 2-H aldehyde). Anal. Calcd for C₃₅H₄₇NO₄: C, 77.03; H, 8.68; N, 2.57%. Found: C, 76.97; H, 8.64; N, 2.55%.

6,6'-methylenebis(2,4-dimethylphenol) (Table 2, Compound **3q**): mp: 105-107 °C; IR (KBr): ν (cm⁻¹) 3424, 3299, 2917, 1609, 1482, 1381, 1286, 1193, 1150, 855. ¹H-NMR (400 MHz, DMSO-d₆) δ (ppm): 2.00 (6H, s, Me), 2.10 (6H, s, Me), 3.74 (2H, s, CH₂), 6.62 (2H, s, OH), 6.68 (2H, s, 3-H DMP), 8.25 (2H, s, 5-H DMP). Anal. Calcd for C₁₇H₂₀O₂: C, 79.65; H, 7.86%. Found: C, 79.62; H, 7.79%.

Acknowledgements

The authors are grateful to University of Kashan for supporting this work by Grant No. 159148/43.

References

1. D. F. Duxbury, *Chem. Rev.*, 1993, **93**, 381-433.
2. P. Rys and H. Zollinger, *Fundamentals of the Chemistry and Application of Dyes*, Wiley-Interscience, 1972.
3. M. S. Shechepinov and V. A. Korshun, *Chem. Soc. Rev.*, 2003, **32**, 170-180.
4. T. Greene and P. Wuts, *Wiley Interscience, New York*, 1999.
5. K. Sumoto, N. Mibu, K. Yokomizo and M. Uyeda, *Chem. Pharm. Bull.*, 2002, **50**, 298-300.
6. M. Okihama and J. Kunitake, *Patent Japan*, 1996, 08,198,790.
7. E. T. Denisov and I. B. Afanas' ev, *Oxidation and antioxidants in organic chemistry and biology*, CRC press, 2010.
8. A. Takeshita, S. Masaki, F. T., T. Tokumaru and A. Marakami, *U. S. Patent*, 1990, 4,912,264.

9. M. Şentürk, İ. Gülçin, A. Daştan, Ö. İrfan Küfrevioğlu and C. T. Supuran, *Bioorg. Med. Chem.*, 2009, **17**, 3207-3211.
10. B. Dimitrios, *Trends Food Sci. Technol.*, 2006, **17**, 505-512.
11. T. Kajiyama and Y. Ohkatsu, *Polym. Degrad. Stab.*, 2002, **75**, 535-542.
12. Y. Liu, S. Su Kim and T. J. Pinnavaia, *J. Catal.*, 2004, **225**, 381-387.
13. I. X. Cerón, R. T. L. Ng, M. El-Halwagi and C. A. Cardona, *J. Food Eng.*, 2014, **134**, 5-15.
14. R. Goossens, M. Smet and W. Dehaen, *Tetrahedron Lett.*, 2002, **43**, 6605-6608.
15. F. A. V. Sullivan and G. Conn, *U. S. Patent*, 1957, 2, 796, 445.
16. Y. A. Gurvich, *U. S. Patent*, 1977, 1,475,973.
17. A. R. Davis and F. A. V. Sullivan, *U. S. Patent*, 1951, 2,538,355.
18. S. Saito, T. Ohwada and K. Shudo, *J. Am. Chem. Soc.*, 1995, **117**, 11081-11084.
19. C. V. Rode, A. C. Garade and R. C. Chikate, *Catal. Surv. Asia*, 2009, **13**, 205-220.
20. K. Shimizu, S. Kontani, S. Yamada, G. Takahashi, T. Nishiyama and A. Satsuma, *Appl. Catal. A: General*, 2010, **380**, 33-39.
21. S. K. Jana, T. Okamoto, T. Kugita and S. Namba, *Appl. Catal. A: General*, 2005, **288**, 80-85.
22. I. Mohammadpoor-Baltork, M. Moghadam, S. Tangestaninejad, V. Mirkhani, K. Mohammadiannejad-Abbasabadi and M. A. Zolfigol, *C. R. Chimie*, 2011, **14**, 934-943.
23. S. Podder, J. Choudhury, U. K. Roy and S. Roy, *J. Org. Chem.*, 2007, **72**, 3100-3103.
24. V. Nair, K. G. Abhilash and N. Vidya, *Org. Lett.*, 2005, **7**, 5857-5859.
25. J. Esquivias, R. Gómez Arrayás and J. C. Carretero, *Angew. Chem. Int. Ed.*, 2006, **45**, 629-633.
26. Z. Li, Z. Duan, J. Kang, H. Wang, L. Yu and Y. Wu, *Tetrahedron*, 2008, **64**, 1924-1930.
27. S. Genovese, F. Epifano, C. Pelucchini and M. Curini, *Eur. J. Org. Chem.*, 2009, **2009**, 1132-1135.
28. M. Kodomari, M. Nagamatsu, M. Akaike and T. Aoyama, *Tetrahedron Lett.*, 2008, **49**, 2537-2540.
29. R. Fareghi-Alamdari, M. Golestanzadeh, F. Agend and N. Zekri, *J. Chem. Sci.*, 2013, **125**, 1185-1195.
30. M. J. Allen, V. C. Tung and R. B. Kaner, *Chem. Rev.*, 2009, **110**, 132-145.
31. H.-J. Shin, K. K. Kim, A. Benayad, S.-M. Yoon, H. K. Park, I.-S. Jung, M. H. Jin, H.-K. Jeong, J. M. Kim, J.-Y. Choi and Y. H. Lee, *Adv. Func. Mater.*, 2009, **19**, 1987-1992.
32. N. R. Wilson, P. A. Pandey, R. Beanland, R. J. Young, I. A. Kinloch, L. Gong, Z. Liu, K. Suenaga, J. P. Rourke, S. J. York and J. Sloan, *ACS Nano*, 2009, **3**, 2547-2556.
33. L. Gao, J. R. Guest and N. P. Guisinger, *Nano Lett.*, 2010, **10**, 3512-3516.
34. X. Tian, F. Su and X. S. Zhao, *Green Chem.*, 2008, **10**, 951-956.
35. M. Kitano, K. Nakajima, J. N. Kondo, S. Hayashi and M. Hara, *J. Am. Chem. Soc.*, 2010, **132**, 6622-6623.
36. H. I. Ryoo, L. Y. Hong, S. H. Jung and D.-P. Kim, *J. Mater. Chem.*, 2010, **20**, 6419-6421.
37. Y. Zhao, H. Wang, Y. Zhao and J. Shen, *Catal. Commun.*, 2010, **11**, 824-828.
38. H. Xiao, Y. Guo, X. Liang and C. Qi, *J. Solid State Chem.*, 2010, **183**, 1721-1725.
39. H. T. Gomes, S. M. Miranda, M. J. Sampaio, A. M. T. Silva and J. L. Faria, *Catal. Today*, 2010, **151**, 153-158.
40. R. Fareghi-Alamdari, M. Golestanzadeh, F. Agend and N. Zekri, *C. R. Chimie*, 2013, **16**, 878-887.
41. R. Fareghi-Alamdari, M. Golestanzadeh, F. Agend and N. Zekri, *Can. J. Chem.*, 2013, **91**, 982-991.
42. M. Toda, A. Takagaki, M. Okamura, J. N. Kondo, S. Hayashi, K. Domen and M. Hara, *Nature*, 2005, **438**, 178-178.
43. S. Sugauma, K. Nakajima, M. Kitano, D. Yamaguchi, H. Kato and S. Hayashi, *J. Am. Chem. Soc.*, 2008, **130**, 12787-12793.
44. M. Hara, T. Yoshida, A. Takagaki, T. Takata, J. N. Kondo, S. Hayashi and K. Domen, *Angew. Chem. Int. Ed.*, 2004, **43**, 2955-2958.
45. A. Onda, T. Ochi and K. Yanagisawa, *Green Chem.*, 2008, **10**, 1033-1037.
46. A. Onda, T. Ochi and K. Yanagisawa, *Top. Catal.*, 2009, **52**, 801-807.
47. H. Naeimi, A. Mohajeri, L. Moradi and A. Rashidi, *J. Nanosci. Nanotechnol.*, 2011, **11**, 8903-8906.
48. L. Moradi, A. Mohajeri, H. Naeimi and A. M. Rashidi, *J. Nanosci. Nanotechnol.*, 2013, **13**, 1923-1926.
49. H. Naeimi and Z. S. Nazifi, *Appl. Catal. A: General*, 2014, **477**, 132-140.
50. H. Naeimi and Z. S. Nazifi, *J. Ind. Eng. Chem.*, 2013, **20**, 1043-1049.
51. H. Naeimi and Z. S. Nazifi, *C. R. Chimie*, 2013, **17**, 41-48.
52. W. S. Hummers and R. E. Offeman, *J. Am. Chem. Soc.*, 1958, **80**, 1339-1339.
53. D. Long, W. Li, L. Ling, J. Miyawaki, I. Mochida and S.-H. Yoon, *Langmuir*, 2010, **26**, 16096-16102.
54. X. Fan, W. Peng, Y. Li, X. Li, S. Wang, G. Zhang and F. Zhang, *Adv. Mater.*, 2008, **20**, 4490-4493.
55. K. N. Kudin, B. Ozbas, H. C. Schniepp, R. K. Prud'homme, I. A. Aksay and R. Car, *Nano Lett.*, 2007, **8**, 36-41.

Graphical abstract

